OPEN ACCESS

Scholars International Journal of Chemistry and Material Sciences

Abbreviated Key Title: Sch Int J Chem Mater Sci
ISSN 2616-8669 (Print) |ISSN 2617-6556 (Online)
Scholars Middle East Publishers, Dubai, United Arab Emirates
Journal homepage: http://saudijournals.com

Original Research Article

Synthesis, Characterization and Application of ZnO/GO/Zeolite-A Nanocomposite in the Sorption of Selected Heavy Metals from Pharmaceutical Effluent

Musah M.[1], Mathew J.T.[1*], Azeh Y[1]

[1]Department of Chemistry, Ibrahim Badamasi Babangida University, Lapai, Niger State, Nigeria

DOI: https://doi.org/10.36348/sijcms.2025.v08i05.003 | **Received:** 11.06.2025 | **Accepted:** 15.08.2025 | **Published:** 13.09.2025

***Corresponding author:** Mathew J.T.
Department of Chemistry, Ibrahim Badamasi Babangida University, Lapai, Niger State, Nigeria

Abstract

In this study, an adsorbent ZnO/GO/Zeolite-A nanocomposite was synthesized and characterized using standard methods for the removal of copper (Cu), iron (Fe), and chromium (Cr) from pharmaceutical effluents. The synthesis involved a multi-step approach comprising hydrothermal synthesis of Zeolite-A, sol-gel formation of ZnO nanoparticles, and incorporation of graphene oxide via ultrasonic dispersion to enhance surface area and functionality. The composite was characterized using X-ray diffraction (XRD), Fourier-transform infrared spectroscopy (FTIR), scanning electron microscopy (SEM), Brunauer–Emmett–Teller (BET) surface analysis, and energy-dispersive X-ray spectroscopy (EDX). The results confirmed a well-integrated, porous nanostructure with high surface area and active functional groups suitable for sorption. Batch sorption experiments were conducted to evaluate the influence of contact time, pH, and temperature. The nanocomposite showed rapid and high sorption efficiency, with maximum removal rates observed at pH 5–6 and equilibrium reached within 60 minutes. The composite exhibits a steady increase from 52.6 % to 100 % efficiency removal of Fe, attributed to its superior adsorption capacity and large specific surface area. The zeolite-A/ZnO/GO consistently shows the best performance compared to individual treatments at all temperatures with Cu, Fe and Cr, showing removal efficiencies of 65.15 % at 50 °C, 75.52 % at 60 °C, and 82.15 % at 70 °C, with synergistic effects becoming more pronounced at elevated temperatures. Thermodynamic studies indicated that the sorption process was spontaneous and endothermic. The integration of ZnO and GO significantly enhanced the adsorption capacity of Zeolite-A due to synergistic effects, making ZnO/GO/Zeolite-A a promising candidate for sustainable treatment of heavy metal-laden pharmaceutical wastewater, contributing to environmental protection and public health improvement.

Keywords: Effluents, Environmental, Heavy Metals, Nanocomposite, Pharmaceutical Effluent.

INTRODUCTION

The release of pharmaceutical effluents containing heavy metals into aquatic environments presents serious threats to both ecological systems and human health. Conventional techniques for eliminating these toxic elements often prove inadequate due to low efficiency and high operational expenses (Etsuyankpa *et al.,* 2024). As a result, nanotechnology has emerged as a viable and innovative solution for treating wastewater. Among the numerous nanomaterials explored, zinc oxide (ZnO) and graphene oxide (GO) have attracted notable interest because of their distinct physicochemical properties and effectiveness in environmental cleanup efforts (Mathew *et al.,* 2024a). ZnO nanoparticles are particularly valued for their large surface area and notable photocatalytic activity, which enhance their ability to adsorb metal ions. Nonetheless, their tendency to cluster together reduces their stability and effectiveness in water. In contrast, GO's layered structure and abundance of oxygenated functional groups give it excellent dispersibility, mechanical strength, and a high surface-to-volume ratio in aqueous systems (Idris *et al.,* 2024).

The combination of ZnO particles with GO sheets leads to the formation of ZnO/GO nanocomposites, which harness the strengths of both materials (Musa *et al.,* 2024; Mititelu *et al.,* 2025). These hybrid materials exhibit improved capacity for heavy metal adsorption due to their expanded surface area and the presence of reactive functional groups that enhance metal ion attachment. Research findings confirm that ZnO/GO composites can efficiently eliminate hazardous metals like cadmium (Cd^{2+}) and lead (Pb^{2+}) from

polluted water. The development and application of these composites for heavy metal sorption from pharmaceutical wastewaters mark a key innovation in the field of water purification. Leveraging the combined capabilities of ZnO and GO, these nanocomposites represent an effective and eco-friendly strategy for reducing metal pollution, thereby safeguarding both the environment and human well-being (Rodríguez *et al.,* 2020; Mathew *et al.,* 2023a).

The anchoring of zinc oxide (ZnO) nanoparticles onto graphene oxide (GO) layers leads to the creation of ZnO/GO nanocomposites, which effectively unify the beneficial attributes of both materials. This composite structure exhibits superior heavy metal adsorption performance, attributed to its enlarged surface area and the functional groups that enhance interaction with metal ions. Research has confirmed the efficacy of ZnO/GO composites in eliminating toxic metals such as cadmium (Cd^{2+}) and lead (Pb^{2+}) from polluted water. Notably, studies have reported impressive adsorption capacities, with values reaching as high as 354.80 mg/g for cadmium ions (Inobeme *et al.,* 2023; Chi *et al.*, 2025).

The development process—spanning synthesis, structural analysis, and practical application—of these ZnO/GO nanocomposites marks a notable breakthrough in the field of wastewater treatment. By exploiting the synergistic characteristics of both ZnO and GO, these materials provide an eco-friendly and highly effective method for addressing heavy metal contamination. Their use supports efforts to protect the environment and ensure public health.

MATERIALS AND METHODS

Sample Collection and Pre-treatment

Clay used in this study was sourced from a natural deposit located in Gbako Local Government Area, Niger State, Nigeria. The pharmaceutical wastewater was obtained from a prominent pharmaceutical company situated in Minna, Niger State. It was collected into a thoroughly cleaned 50-litre container that had been rinsed with a dilute solution of nitric acid (HNO_3). The collected wastewater samples were then transported to the laboratory for analysis of selected physicochemical properties.

Synthesis of zeolite-A

The purified kaolin sample underwent calcination at 600 °C for 12 hours to produce metakaolin, which served as the precursor for synthesizing zeolite A. The synthesis followed a hydrothermal method, characterized as a multiphase reaction and crystallization process, as highlighted by Pereira *et al.,,,* (2019). This technique typically involves the coexistence of a liquid phase along with both amorphous and crystalline solids. Zeolite A was obtained by treating the metakaolin with a 5.0 mol/dm³ sodium hydroxide (NaOH) solution, using a NaOH-to-metakaolin molar ratio of 8:1, assuming the chemical composition of metakaolin to be $Al_2Si_2O_7$. The reaction mixture was continuously stirred magnetically and maintained at 80 °C for 24 hours. After synthesis, the product was thoroughly rinsed with deionized water and subsequently dried at 110 °C.

Synthesis of graphene oxide (GO)

Graphene oxide (GO) particles were synthesized using the chemical vapor deposition (CVD) technique, following the procedure outlined by Saeed *et al.,* (2020). The key variables examined in the process were the reaction temperature and the flow rate of the carbon source. Initially, nitrogen (N_2) gas was purged through the reactor for 15 minutes to eliminate residual oxygen. Subsequently, a nitrogen-hydrogen (N_2/H_2) mixture at a flow rate of 1 L/min was introduced to reduce surface copper oxides on the substrate. Acetylene gas was then introduced into the reactor at a steady flow rate for 1 minute. Following this, the gas injection was halted to initiate graphene growth using the trapped gases at varying temperatures. The system was then cooled under a nitrogen atmosphere with a controlled rate of 8 °C per minute.

Synthesis of zinc oxide nanoparticles via sol-gel method

Zinc oxide nanoparticles were synthesized using a modified sol-gel technique. Precisely 50 grams of zinc acetate dihydrate [$Zn(C_2H_3O_2)_2{\cdot}2H_2O$] was weighed into a 250 cm³ beaker, followed by the addition of approximately 100.0 cm³ of deionized water. The mixture was continuously stirred with a magnetic stirrer for 30 minutes at a speed of 150 rpm. A 0.5 M sodium hydroxide (NaOH) solution was then gradually added drop by drop until the pH values of 6, 8, 10, and 12 were achieved. Afterward, the solution was stirred for an additional 5 minutes, leading to the formation of a precipitate. This precipitate was collected using Whatman No. 1 filter paper and thoroughly washed with deionized water and ethanol to remove any remaining unreacted materials. The washed product was then dried in an oven at 105 °C for 24 hours and subsequently calcined at 450 °C in a furnace to yield the final ZnO nanoparticles (Mathew *et al.*, 2023b).

Synthesis of zeolite A/graphene oxide

The zeolite A/ZnO/graphene oxide composite was synthesized using the wet impregnation technique. Equal masses of each nanomaterial were dispersed in 100 cm³ of deionized water and stirred continuously for one hour. The resulting mixture was then placed in an oven and dried at 105 °C until complete dryness was achieved.

Heavy Metal Determination

About 50 cm³ of the wastewater sample was transferred into a 100 cm³ beaker. To this, 15 cm³ of concentrated nitric acid and 10 cm³ of 50% hydrochloric acid were added. The mixture was heated on a hot plate, after which an additional 7 cm³ of 50% hydrochloric acid was introduced. Heating continued for 10 minutes. The

solution was then allowed to cool before adding deionized water. Filtration was carried out using Whatman No. 42 filter paper into a 100 cm^3 Pyrex volumetric flask. The volume was adjusted to the mark with deionized water and the sample was preserved for heavy metal analysis, including zinc (Zn), lead (Pb), cadmium (Cd), and chromium (Cr), using a Perkin Elmer 200 Atomic Absorption Spectrophotometer, in line with the method outlined by Mathew *et al.,* (2024b).

Characterization of Nanoadsorbents

Zeolite-A nanoparticles were analyzed using a range of advanced characterization techniques, including X-ray diffraction (XRD), high-resolution scanning electron microscopy (HRSEM), high-resolution transmission electron microscopy (HRTEM) combined with energy-dispersive X-ray spectroscopy (EDS), and Brunauer–Emmett–Teller (BET) surface area analysis (Musah *et al.,* 2024).

Batch Adsorption Process

Batch adsorption experiments, including the investigation of contact time, adsorbent dosage, and temperature effects, were conducted following the standard procedures outlined by Mathew *et al.,* (2024).

Adsorption Isotherms

The isothermal experimental data were evaluated using the Langmuir and Freundlich adsorption models, as described by Mathew *et al.,* (2024) and Musah *et al.,* (2022).

Adsorption Kinetics

The adsorption kinetics of metal ions onto the nanocomposites from wastewater were analyzed using the pseudo-first-order and pseudo-second-order kinetic models (Alhalili and Abdelrahman, 2024).

RESULT AND DISCUSSION

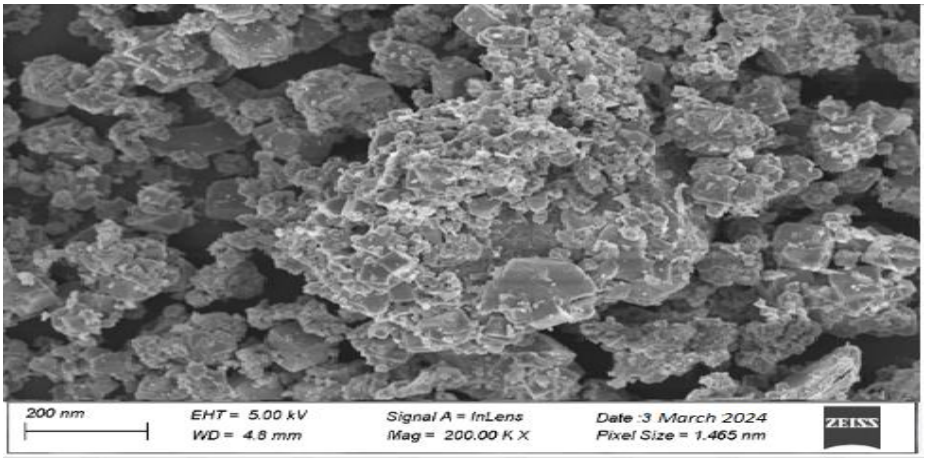

Figure 1: HRSEM images of Zn/GO

The high-resolution scanning electron microscopy (HRSEM) image of the zeolite-A/ZnO/graphene oxide nanocomposite, as illustrated in Figure 1, displays detailed microstructural features. Zeolite-A is identified within the composite as fine, crystalline particles exhibiting a consistent and orderly shape. Ashfaq *et al.,* (2022), for instance, examined the controlled formation of TiO_2/zeolite nanocomposites, noting how variations in surface and chemical characteristics relate to zeolite morphology within the material. Similarly, Han (2023) explored functionalized nano-zeolite-based composites, stressing the role of zeolite structure in improving attributes like thermal performance.

Dispersed throughout the matrix, zinc oxide (ZnO) nanoparticles appear as small, non-uniform particles that either attach to the graphene oxide surfaces or are embedded within the zeolite-A framework. Chaturvedi and Kundu (2022) highlighted that enhanced nanocomposite activity can be attributed to its porous texture and active functional groups, which likely promote effective ZnO dispersion. Amini (2023) further demonstrated the integration of MoS_2@Zeolite X nanocomposites into thin-film membranes, revealing how zeolite materials can be incorporated into selective membrane layers, supporting ZnO embedding or surface interaction with graphene oxide.

Graphene oxide, meanwhile, presents itself as flat, layered sheets—often slightly wrinkled or folded—serving as a structural platform for supporting both zeolite-A and ZnO nanoparticles. According to Xu *et al.,* (2008), these sheets possess distinct nanoscale features and are excellent frameworks for forming hybrid structures and distributing nanoparticles uniformly. Overall, the HRSEM image reflects a uniformly distributed and tightly connected network of zeolite-A, ZnO, and graphene oxide, which collectively contribute to the composite's mechanical robustness and functional enhancement.

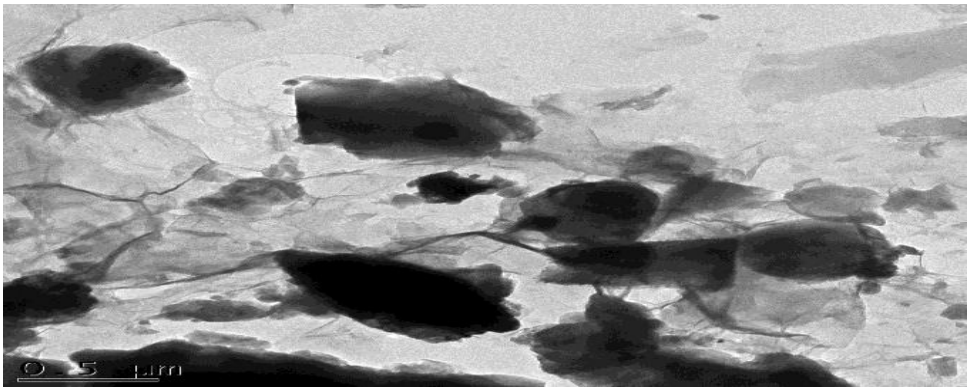

Figure 2: HRTEM images of zeolite-A/ZnO/GO

The high-resolution transmission electron microscopy (HRTEM) analysis of the zeolite-A/ZnO/graphene oxide (GO) nanocomposite displays clearly defined structural features and visible lattice fringes, indicating a crystalline framework and effective dispersion of the constituent materials (Fig. 2). Elemental analysis using energy-dispersive X-ray spectroscopy (EDX), shown in Fig. 3, confirms the presence of elements corresponding to zeolite-A, ZnO, and GO, providing evidence of successful synthesis and uniform integration of the components within the composite. Similar observations were reported by Salih *et al.,* (2016), who used HRTEM to examine a ZnO/GO nanocomposite and identified well-formed ZnO nanocrystals distributed across the GO surface. In addition, Raizada *et al.,* (2017) employed EDX, SEM, and TEM to study a ZnO/$ZnWO_4$/activated carbon (AC) composite, confirming both effective synthesis and consistent distribution of the composite's individual phases.

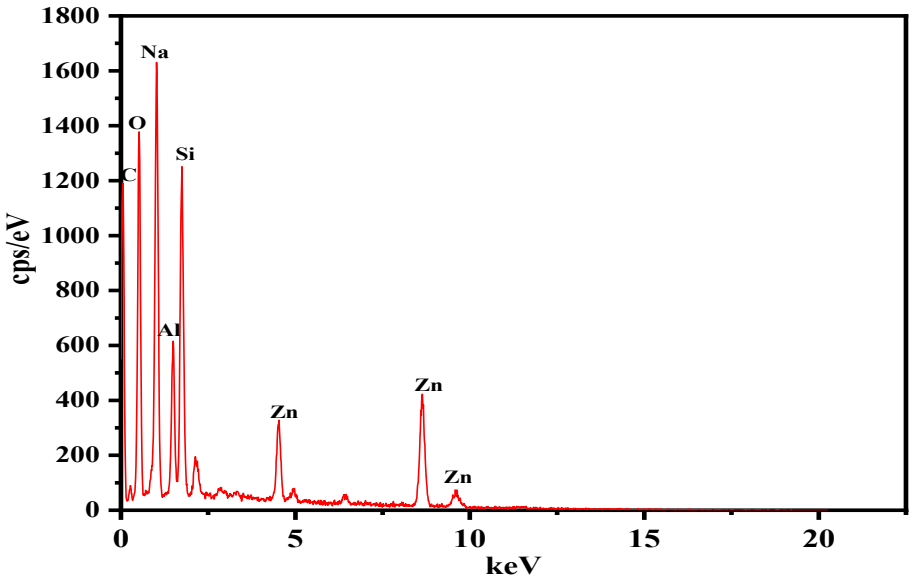

Figure 3: EDX spectra of zeolite-A/ZnO/GO

The X-ray diffraction (XRD) pattern of the zeolite-A/ZnO/graphene oxide (GO) nanocomposite reveals distinct diffraction peaks attributable to each individual component (Fig. 4). Zeolite-A displays sharp reflections around 2θ = 9.7° and 22.5°, indicative of its crystalline framework. ZnO presents notable peaks near 2θ values of 31.8°, 34.4°, and 36.3°, which correspond to its hexagonal wurtzite phase. Graphene oxide, due to its less ordered structure, typically shows a broad peak in the 2θ range of 10–25°, often overlapping with signals from other materials in the composite. Consequently, the XRD spectrum of the composite exhibits a superimposition of these characteristic peaks, confirming the coexistence and relative crystallinity of zeolite-A, ZnO, and GO within the nanomaterial (Ali *et al.,* 2022).

Earlier investigations have noted that the crystalline intensity of zeolite tends to decline upon integration with graphene oxide, although the structural integrity of the zeolite framework is maintained when reduced graphene oxide is used, as verified by XRD (Jeong *et al.,* 2024). Moreover, XRD analysis of reduced graphene oxide/ZnO composites has demonstrated

enhancements in crystallinity linked to increased crystallite size, extended Zn–O bond length, and enlarged unit cell dimensions as the ZnO content rises (Elshypany *et al.,* 2021). Additionally, studies on ZnO/graphene oxide nanocomposites have reported distinct, sharp peaks corresponding to the crystalline wurtzite ZnO phase and reduced graphene oxide, reinforcing the composite's structural configuration (Boukhoubza *et al.,* 2020).

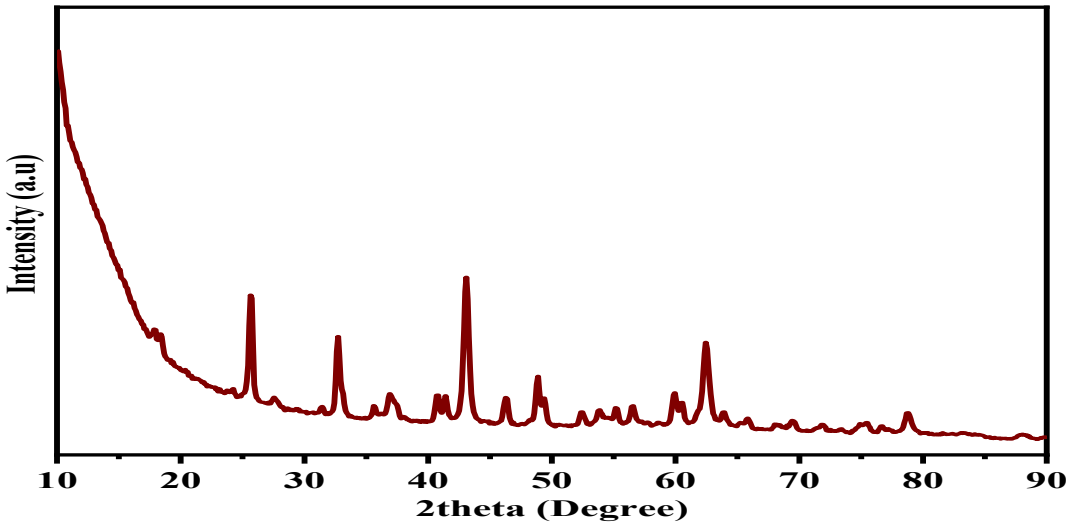

Figure 4: XRD pattern of zeolite-A/ZnO/GO

The Brunauer–Emmett–Teller (BET) analysis, as presented in Table 1, provides valuable insights into the surface characteristics of the zeolite-A/ZnO/graphene oxide (GO) composite. Notably, the composite exhibits a surface area of 121.02 m^2/g, reflecting a synergistic improvement likely resulting from the integration of the individual structural components and their interactions. Among the materials examined, the composite also features the smallest pore diameter at 2.761 nm, which may be attributed to increased interlayer spacing or the presence of finer mesopores.

Vu *et al.,* (2016) explored the synthesis of micro/mesoporous zeolitic composites (MZCs), underscoring the growing relevance of hierarchical zeolite structures. The observed small pore size in the zeolite-A/ZnO/GO composite suggests the presence of both microporous and mesoporous features. Furthermore, the composite demonstrates the highest pore volume, recorded at 0.3812 cc/g, indicating a greater cumulative pore capacity likely resulting from the integration of diverse pore architectures.

Table 1: Summary of BET results of zeolite-A/ZnO/GO

Adsorbent	Surface area (m^2/g)	Pore size (nm)	Pore volume (cc/g)
Zeolite-A/ZnO/GO	121.02	2.761	0.3812

Table 2 presents the analysis of selected physicochemical characteristics of pharmaceutical wastewater. The sample exhibited a pale brown coloration, indicating the presence of dissolved organic substances and byproducts of pharmaceutical degradation. This coloration is often attributed to organic dyes and chemical compounds commonly found in pharmaceutical effluents. The pH value recorded was 5.42, revealing a mildly acidic nature. This finding aligns with previous studies by Liu *et al.,* (2023) and Satar *et al.,* (2023), which note that acidic pH conditions can influence solubility and chemical speciation, thereby affecting biological treatment efficiency. Regulatory standards, such as those by the USEPA, recommend a pH range of 6.5–8.5, suggesting that pH modification is necessary before discharge (Onadeji, 2024; Zhao, 2024). It is well-documented that variations in pH impact aquatic ecosystems (Satar *et al.,* 2023). Additionally, high values of pH, COD, and TSS are typically linked to elevated levels of proteins, fats, and carbohydrates, which contribute to water pollution (Adriansyah, 2023). The use of neutralizing agents like calcium hydroxide has been shown to enhance pollutant removal efficiency (Chen *et al.,* 2022).

The measured Chemical Oxygen Demand (COD) was 138.51 mg/L, which is consistent with findings that identify COD as a key indicator of the oxygen required to chemically oxidize organic matter in water (Yu *et al.,* 2022). The observed COD level reflects a moderate organic load, potentially treatable via biological means, though additional processes may be necessary for thorough remediation. The USEPA threshold for COD in discharged wastewater is 410 mg/L. The Biochemical Oxygen Demand (BOD) was recorded at 40.02 mg/L, signifying the oxygen needed by

microbes to break down biodegradable organic material—a parameter essential for assessing suitability for biological treatment (Damiao, 2024).

The Total Dissolved Solids (TDS) concentration was 301 mg/L, indicating the presence of both organic and inorganic dissolved substances. This value remains within the USEPA permissible limit of 500 mg/L but suggests attention to dissolved salts and compounds that may impact treatment and reuse options. Chloride levels were markedly high at 4916 mg/L, far exceeding the regulatory maximum of 250 mg/L, and likely originating from chlorinated substances or chemical formulations, thus necessitating specialized remediation to mitigate water quality deterioration.

Nitrate concentration stood at 60.92 mg/L, significantly surpassing the USEPA limit of 10 mg/L. This may reflect contamination from pharmaceutical or nitrogen-rich waste, which poses environmental risks such as eutrophication and public health concerns. Phosphate content measured at 38.75 mg/L, suggesting input from detergents or other industrial sources; uncontrolled phosphate levels are known contributors to eutrophication in natural water bodies.

Additionally, the sample contained heavy metals including Cadmium (Cd), Copper (Cu), Chromium (Cr), Iron (Fe), Manganese (Mn), and Nickel (Ni) in various concentrations. These elements are hazardous to aquatic organisms, bioaccumulate in sediments, and present long-term ecological risks.

Table 2: Some physicochemical parameters of pharmaceutical wastewater

Parameter	Sample	USEPA (Permissible limit)
Colour	Pale brown	
pH	5.42	6.5-8.5
COD (mg/L)	138.51	410
BOD (mg/L)	40.02	
TDS (mg/L)	301	500
Chloride (mg/L)	4916	250
Nitrate (mg/L)	60.92	10
Phosphate (mg/L)	38.75	
Cd (mg/L)	0.001	0.005
Cu (mg/L)	3.53	1.0
Cr (mg/L)	2.09	0.10
Fe (mg/L)	2.86	0.30
Mn (mg/L)	0.38	0.05
Ni (mg/L)	0.02	

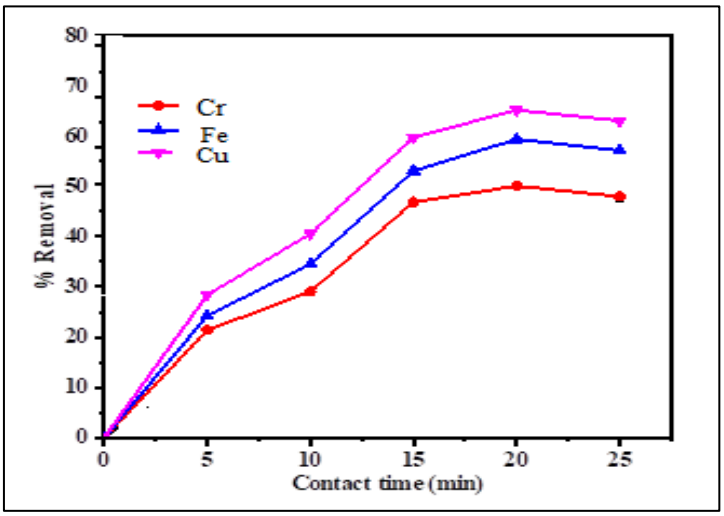

Figure 5: Effect of contact time on the removal of (a) Cu (b) Fe and (c) Cr ions using zeolite-A/ZnO/GO

Figure 5 illustrates the adsorption behavior of Cu, Cr, and Fe ions from pharmaceutical wastewater using the zeolite-A/ZnO/GO nanocomposite at various contact times (0, 5, 10, 15, 20, and 25 minutes). The removal efficiency for Cu ions increases progressively with time, peaking around 20 minutes, after which it stabilizes or slightly decreases—likely due to saturation of available active sites on the adsorbent surface. A similar trend is observed for Fe ions, where removal efficiency improves over time, particularly within the first 10 minutes, and levels off near the 20-minute mark. This behavior is associated with surface interactions and the adsorption mechanism specific to Fe ions.

Compared to Cr, the nanocomposite demonstrates higher efficiency in removing Fe and Cu, especially during the initial contact periods. Notably, Cu shows the most significant enhancement in removal performance with increasing contact time, attributed to the nanocomposite's large surface area and strong adsorption affinity. The ZnO/GO/zeolite-A hybrid exhibits optimal removal efficiency for Cu, particularly within the 15–20-minute range, suggesting that the synergistic integration of these materials significantly boosts their collective adsorption performance, especially in removing Fe and Cu ions from pharmaceutical wastewater.

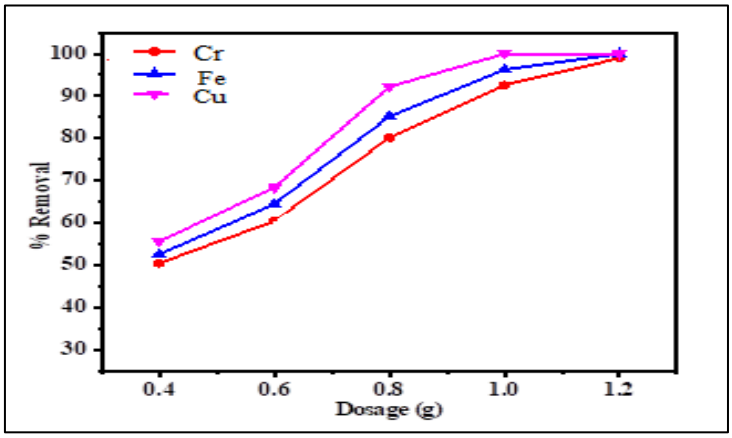

Figure 6: Effect of dosage on the removal of (a) Cu (b) Fe and (c) Cr ions using zeolite-A/ZnO/GO

Figure 6 displays the removal efficiency of Cu, Fe, and Cr ions from wastewater using the zeolite-A/ZnO/GO nanocomposite across varying adsorbent dosages. The removal of Cu ions improves progressively with increasing dosage—from 43.51% at 0.4 g to 94.16% at 1.2 g—highlighting the role of increased surface area in enhancing adsorption. Similarly, Cr ions exhibit a rise in removal efficiency from 50.48% to 98.96% within the same dosage range, attributed to the composite's high reactivity and surface characteristics.

Fe ion removal efficiency also shows a consistent upward trend, increasing from 52.6% to complete removal (100%) as dosage increases, reflecting the nanocomposite's strong adsorption capacity and extensive specific surface area. At the highest dosage of 1.2 g, the ZnO/GO/zeolite-A composite achieves 100% removal efficiency, indicating the synergistic integration of the three components significantly improves adsorption performance over the individual materials.

Overall, the enhancement in removal efficiency with increasing dosage is due to the greater number of available active sites and expanded contact area for adsorption. The composite consistently outperforms its individual constituents, underscoring the advantage of material synergy in improving wastewater treatment efficacy.

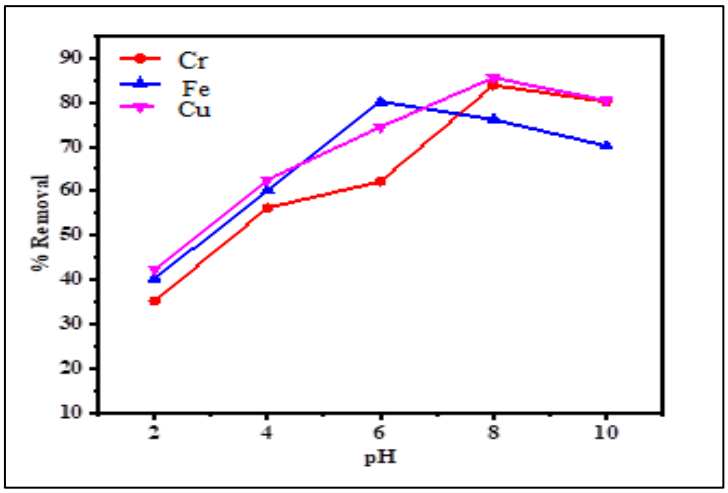

Figure 7: Effect of pH on the removal of (a) Cr (b) Fe and (c) Cu ions using zeolite-A/ZnO/GO

Figure 7 illustrates the influence of pH on the removal efficiency of Cu, Fe, and Cr ions using the ZnO/GO/zeolite-A nanocomposite. As pH increases from 2 to 10, there is a clear upward trend in removal efficiency for all three metal ions. At pH 2, the composite eliminates approximately 39.16 % of Cu ions, which

increases significantly to 87.1 % at pH 10. This trend indicates enhanced adsorption at higher pH levels, likely due to improved surface reactivity and ion exchange interactions.

For Fe ions, removal efficiency also rises with pH, from 35.16 % at pH 2 to 80.15 % at pH 10 suggesting that the surface charge and chemical interactions of the composite favor Fe ion binding at more alkaline conditions. In the case of Cr ions, removal efficiency begins at 40.18 % at low pH and increases to 80.2 % by pH 10, benefiting from the material's high surface area and reactive functional groups.

The ZnO/GO/zeolite-A nanocomposite shows superior performance across pH levels compared to its individual constituents, with Cu ion removal starting at 42.43 % at pH 2 and peaking at 85.63 % at pH 8. This enhanced performance is attributed to the synergistic integration of the three components, optimizing adsorption where each material demonstrates optimal efficiency.

The observed pH dependence can be explained by changes in surface charge, the ionization state of functional groups, and shifts in metal ion speciation in solution. As highlighted by Li *et al.,* (2022), pH plays a crucial role in determining the adsorption and desorption behavior of ionizable compounds on carbon-based materials, reinforcing its importance in wastewater treatment processes.

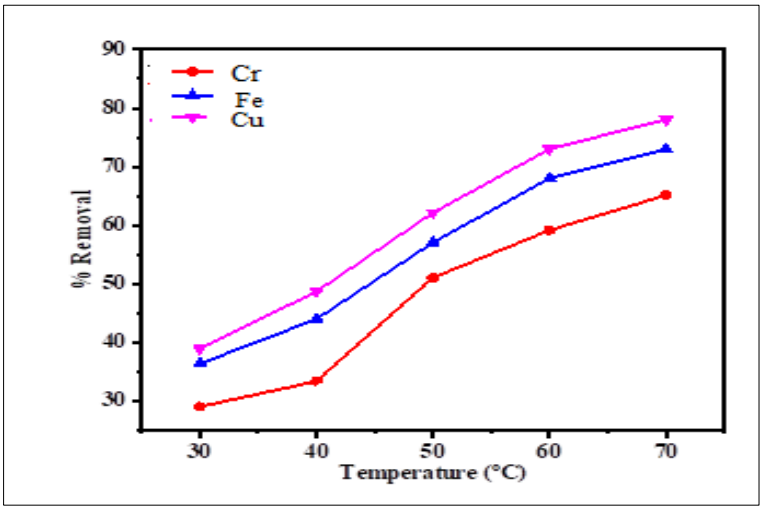

Figure 8: Effect of temperature on the removal of (a) Cu (b) Fe and (c) Cr ions using zeolite-A/ZnO/GO

At elevated temperatures (50 °C, 60 °C, and 70 °C), the removal efficiency for Cu ions progressively increases, reaching 49.06 % at 50 °C, 56.76 % at 60 °C, and peaking at 73.7 % at 70 °C. This trend highlights the role of temperature in enhancing adsorption kinetics. The nanocomposite exhibits a consistent rise in performance with increasing temperature, achieving 60.45 % removal at 50 °C, 67.18 % at 60 °C, and 75.45 % at 70 °C, suggesting a strong temperature-dependent enhancement in its adsorption behavior.

For Fe ions, removal remains efficient across all elevated temperatures, with values of 62.75 % at 50 °C, 70.61 % at 60 °C, and 80.4 % at 70 °C, indicating a thermally responsive adsorption process. Similarly, Cr ion removal also improves as temperature rises, demonstrating the composite's high sensitivity to thermal activation.

Among all tested materials, the zeolite-A/ZnO/GO nanocomposite consistently achieves superior removal efficiencies for Cu, Fe, and Cr ions. At 50 °C, 60 °C, and 70 °C, it records 65.15 %, 75.52 %, and 82.15 % removal, respectively. These results confirm that the synergistic interaction among the composite's components becomes increasingly effective at higher temperatures, leading to improved adsorption capacity across the board.

Table 3: Isotherm parameters on the removal of Cr, Fe and Cu ion from wastewater using zeolite-A/ZnO/GO

Metal ion	Langmuir			Freundlich			Temkin		
	q_e	K_L	R^2	K_F	$\frac{1}{n}$	R^2	a	b	R^2
Cr	82.15	0.907	0.9998	4.215	0.570	0.9914	6.705	5.163	0.9902
Fe	71.08	0.815	0.9956	3.057	0.611	0.9890	4.056	2.201	0.9845
Cu	60.05	0.723	0.9930	2.816	0.672	0.9873	3.803	1.905	0.9801

Table 3 presents the isotherm analysis data for the ZnO/GO/zeolite-A composite in removing Cr, Fe, and Cu ions from dye-contaminated wastewater. The composite exhibits markedly superior adsorption capacities—reaching up to 82.15 mg/g—exceeding those of its individual components. This improvement reflects the synergistic interaction among ZnO, graphene oxide, and zeolite-A. The adsorption behavior aligns closely with the Langmuir isotherm model, as indicated by high correlation coefficients ($R^2 > 0.99$), suggesting efficient monolayer adsorption on a homogeneous surface. Additionally, the Temkin isotherm model also provides strong fits ($R^2 \approx 0.98–0.99$), indicating uniform surface energies and robust adsorbate–adsorbent interactions. These findings underscore the composite's enhanced binding affinity and adsorption performance, attributed to the integrated functionality of its constituent materials.

Table 4: Kinetic parameters on the removal of Cr, Fe and Cu ion from wastewater using zeolite-A/ZnO/GO

Material	Metal ion	Pseudo-first-order			Pseudo-second-order			Elovich		
		q_e	k_1	R^2	q_e	k_2	R^2	a	b	R^2
Zeolite-A/ZnO/GO	Cr	58.60	0.194	0.9381	78.76	2.513	0.9990	8.90	1.86	0.9510
	Fe	39.45	0.0960	0.9052	69.35	2.191	0.9968	4.04	0.88	0.8818
	Cu	30.08	0.0751	0.8950	57.16	1.962	0.9954	3.40	0.79	0.8706

As shown in Table 4, the Elovich kinetic model parameters (a and b) indicate relatively slow initial adsorption rates (b) but highlight a substantial overall adsorption capacity (a) over time. Although the model demonstrates moderate to high correlation coefficients (R^2), they are slightly lower than those observed for the pseudo-second-order model, implying that the Elovich model provides an adequate, though not the most precise, and representation of the adsorption behavior. This suggests that while chemisorption plays a role, it may not fully describe the kinetics involved. Similar findings have been reported by N'Diaye (2022), He *et al.,* (2015), and Harrache and Abbas (2022), who compared the Elovich model to other kinetic models and found that it often yields fairly good, but not superior, fits. The zeolite-A/ZnO/GO nanocomposite demonstrates remarkable efficiency in adsorbing Cr, Fe, and Cu ions from pharmaceutical wastewater. Compared to the individual materials, the composite shows enhanced adsorption kinetics and capacity. The pseudo-second-order model offers the best fit for the experimental data, reinforcing that chemisorption is likely the dominant mechanism controlling metal ion uptake by the composite.

CONCLUSION

The study showed that zeolite A/ZnO/GO nanocomposites exhibited remarkable effectiveness in eliminating various pharmaceutical contaminants, including heavy metals, dyes, and organic substances, when operated under optimal conditions. Key parameters such as contact duration, contaminant concentration, pH level, and temperature had a notable impact on the efficiency of pollutant removal. The exceptional performance of the nanocomposite is linked to the large surface area and porous structure of zeolite A, the photocatalytic capabilities of ZnO, and the excellent electrical conductivity and adsorption strength of graphene oxide. The combined effects of these materials facilitated efficient pollutant adsorption, degradation, and improved catalytic reactions under visible light exposure.

ACKNOWLEDGMENTS

In appreciation for funding this study, the authors are grateful to the Tertiary Education Trust Fund (TETFund) and the management of Ibrahim Badamasi Babangida University, Lapai, Niger State, Nigeria for fostering an enabling research environment.

REFERENCES

- Adriansyah, E. (2023). Advanced treatment of tofu wastewater using multilevel filtration and TiO_2 photocatalysis as promising approach for effective wastewater remediation. *Jurnal Presipitasi Media Komunikasi Dan Pengembangan Teknik Lingkungan*, 20(3), 560-571. https://doi.org/10.14710/presipitasi.v20i3.560-571
- Alhalili, Z., & Abdelrahman, E. A. (2024). Efficient removal of Zn(II) ions from aqueous media using a facilely synthesized nanocomposite based on chitosan Schiff base. *Scientific Reports*, 14, 17598. https://doi.org/10.1038/s41598-024-68745-5
- Ali, A., Chiang, Y. W., & Santos, R. M. (2022). X-ray Diffraction Techniques for Mineral Characterization: A Review for Engineers of the Fundamentals, Applications, and Research Directions. *Minerals*, *12*(2), 205. https://doi.org/10.3390/min12020205
- Amini, M., Nikkhoo, M., Bagherzadeh, M., Ahadian, M. M., Bayrami, A., Naslhajian, H., … & Karamjavan, M. H. (2023). High-performance novel mos2@zeolite x nanocomposite-modified thin-film nanocomposite forward osmosis membranes: a study of desalination and antifouling performance. *ACS Applied Materials &Amp; Interfaces*, 15(33), 39765-39776. https://doi.org/10.1021/acsami.3c03481
- Ashfaq, M. H., Shahid, S., Javed, M., Iqbal, S., Hakami, O., Aljazzar, S. O. & Somaily, H. H. (2022). Controlled growth of tio2/zeolite nanocomposites for simultaneous removal of ammonium and phosphate ions to prevent

eutrophication. *Frontiers in Materials*, 9. https://doi.org/10.3389/fmats.2022.1007485

- Boukhoubza, I., Khenfouch, M., Achehboune, M., Leontie, L., Galca, A. C., Enculescu, M., Carlescu, A., Guerboub, M., Mothudi, B. M., Jorio, A., & Zorkani, I. (2020). Graphene Oxide Concentration Effect on the Optoelectronic Properties of ZnO/GO Nanocomposites. *Nanomaterials*, *10*(8), 1532. https://doi.org/10.3390/nano10081532
- Chaturvedi, A. and Kundu, P. P. (2022). Co-doped zeolite–go nanocomposite as a high-performance orr catalyst for sustainable bioelectricity generation in air-cathode single-chambered microbial fuel cells. *ACS Applied Materials &Amp; Interfaces*, 14(29), 33219-33233. https://doi.org/10.1021/acsami.2c07638
- Chen, D., Zhao, M., Tao, X., Ma, J., Liu, A., & Wang, M. (2022). Exploration and optimisation of high-salt wastewater defluorination process. *Water*, 14(23), 3974. https://doi.org/10.3390/w14233974
- Chi, H., Cao, P., Shi, Q., Song, C., Lv, Y., & Peng, T. (2025). Photocatalytic Degradation of Ciprofloxacin by GO/ZnO/Ag Composite Materials. *Nanomaterials*, *15*(5), 383. https://doi.org/10.3390/nano15050383
- Damiao, S. M. E. and Sequihod, C. D. (2024). Water quality of tago river. *Cognizance Journal of Multidisciplinary Studies*, 4(3), 216-220. https://doi.org/10.47760/cognizance.2024.v04i03.019
- Elshypany, R., Selim, H., Zakaria, K., Moustafa, A. H., Sadeek, S. A., Sharaa, S. I., Raynaud, P., & Nada, A. A. (2021). Magnetic ZnO Crystal Nanoparticle Growth on Reduced Graphene Oxide for Enhanced Photocatalytic Performance under Visible Light Irradiation. *Molecules*, *26*(8), 2269. https://doi.org/10.3390/molecules26082269
- Etsuyankpa, M. B., Augustine, A. U., Musa, S. T., Mathew, J. T., Ismail, H., Salihu, A. M., Mamman, A (2024). An Overview of Wastewater Characteristics, Treatment and Disposal: A Review. *Journal of Applied Science and Environmental Management,* 28 (5) 1553-1572. Doi: https://dx.doi.org/10.4314/jasem.v28i5.28
- Han, B., Dai, J., Zhao, W., Song, W., Sun, Z., & Wang, X. (2023). Preparation and space charge properties of functionalized zeolite/crosslinked polyethylene composites with high thermal conductivity. *Polymers*, 15(22), 4363. https://doi.org/10.3390/polym15224363
- Harrache, Z. and Abbas, M. (2022). Elimination of a cationic dye in aqueous solution by adsorption on activated carbon: optimization of analytical parameters, modeling and thermodynamic study. *Journal of Engineered Fibers and Fabrics*, 17, 155892502211343. https://doi.org/10.1177/15589250221134343
- He, Z., Liu, R., Liu, H., & Qu, J. (2015). Adsorption of sb(iii) and sb(v) on freshly prepared ferric hydroxide (feoxhy). *Environmental Engineering Science*, 32(2), 95-102. https://doi.org/10.1089/ees.2014.0155
- Idris A. Y., Elele U. U. and Mathew, J. T. (2024). Preparation and characterization of MoO_3 nanoparticles for the photocatalytic degradation of dyeing wastewater. *Science World Journal Vol.* 19(4), 1006-1011. https://dx.doi.org/10.4314/swj.v19i4.14
- Inobeme, A., Mathew, J. T., Adetunji, C.O., Ajai, A.I., Inobeme, J. Maliki, M., Okonkwo, S., Adekoya, M.A., Bamigboye, M.O., Jacob, J.O., Eziukwu, C.A. (2023). Recent advances in nanotechnology for remediation of heavy metals. *Environmental Monitoring Assessment*, 195(111), 1-24. https://doi.org/10.1007/s10661-022-10614-7.
- Jeong, S.-W., Oh, B. I., Chang, E. S., Park, J.-A., & Kim, H.-K. (2024). Lithiophilic Reduced Graphene Oxide/Carbonized Zeolite Imidazolate Framework-8 Composite Host for Stable Li Metal Anodes. *Materials*, *17*(17), 4300. https://doi.org/10.3390/ma17174300
- Li, J., Gao, M., Yan, W., & Yu, J. (2023). Regulation of the Si/Al ratios and Al distributions of zeolites and its impact on properties. *Chemical Science*.
- Mathew, J. T., Musah, M., Azeh, Y. & Muhammed, M. (2024a). Development of Fe3O4 Nanoparticles for the Removal of Some Toxic Metals from Pharmaceutical Wastewater. Caliphate Journal of Science & Technology (CaJoST), 6(1), 26-34. Doi: https://dx.doi.org/10.4314/cajost.v6i1.4
- Mathew, J. T., Musah, M., Azeh, Y. & Musa, M. (2024b). Removal of Some Toxic Metals from Pharmaceutical Wastewater Using Geopolymer/Fe_3O4/ZnO nanocomposite: Isotherm, Kinetics and Thermodynamic Studies. *Confluence University Journal of Science and Technology*, 1(1): 50-58. Doi: 10.5455/CUJOSTECH.240706.
- Mathew, J. T., Musah, M., Azeh, Y. & Muhammed, M. (2023a). Adsorptive Removal of Selected Toxic Metals from Pharmaceutical Wastewater using Fe_3O_4/ZnO Nanocomposite, *Dutse Journal of Pure and Applied Sciences*, 9(4a), 236- 248. https://dx.doi.org/10.4314/dujopas.v9i4a.22.
- Mathew, J. T., Musah, M., Azeh, Y. & Muhammed, M. (2023b). Kinetic Study of Heavy Metals Removal from Pharmaceutical Wastewater Using Geopolymer/Fe_3O_4 Nanocomposite. *Bima Journal of Science and Technology*, 7(4), 152- 163. Doi: 10.56892/bima.v7i4.539.
- Mititelu, M., Neacșu, S. M., Busnatu, Ș. S., Scafa-Udriște, A., Andronic, O., Lăcraru, A. E., Ioniță-Mîndrican, C.-B., Lupuliasa, D., Negrei, C., & Olteanu, G. (2025). Assessing Heavy Metal Contamination in Food: Implications for Human Health and Environmental Safety. *Toxics*, *13*(5), 333. https://doi.org/10.3390/toxics13050333
- Musa, A. V., Musah, M. and Mathew, J. T. (2024). Production and characterization of Zeolite-A

nanoparticles for the treatment of pharmaceutical wastewater. *Science World Journal Vol.* 19(4), 987-993. https://dx.doi.org/10.4314/swj.v19i4.11

- Musah, M., Matthew, J. T., Azeh, Y., Badeggi, U. M., Muhammad, A. I., Abu, L. M., Okonkwo, P. T., & Muhammad, K. T. (2024). Preparation and Characterization of Adsorbent from Waste Shea (*Vitellaria paradoxa*) Nut Shell. *FUDMA Journal of Sciences*, 8(2), 338 - 344. https://doi.org/10.33003/fjs-2024-0802-2370.
- Musah, M., Azeh, Y., Mathew, J. T., Umar, U. M., Abdulhamid, Z. & Muhammad, A. I. (2022). Adsorption kinetics and isotherm models: A Review. *Caliphate Journal of Science and Technology*, 4(1),20-26.
- N'diaye, A. (2022). Nonlinear analysis of the kinetics and equilibrium for adsorptive removal of paranitrophenol by powdered activated carbon. *Asean Journal of Science and Engineering*, 3(3), 271-280. https://doi.org/10.17509/ajse.v3i3.49136
- Onadeji, A. (2024). Response surface methodology optimization of the effect of ph, contact time, and microbial concentration on chemical oxygen removal potential of vegetable oil industrial effluents. *Water Environment Research*, 96(1). https://doi.org/10.1002/wer.10963
- Pereira, P. M., Ferreira, B. F., Oliveira, N. P., Nassar, E. J., Ciuffi, K. J., Vicente, M. A., Trujillano, R., Rives, V., Gil, A., Korili, S., & De Faria, E. H. (2018). Synthesis of Zeolite A from Metakaolin and Its Application in the Adsorption of Cationic Dyes. *Applied Sciences*, *8*(4), 608. https://doi.org/10.3390/app8040608
- Rodríguez, C., Tapia, C., Leiva-Aravena, E., & Leiva, E. (2020). Graphene Oxide–ZnO Nanocomposites for Removal of Aluminum and Copper Ions from Acid Mine Drainage Wastewater. *International Journal of Environmental Research and Public Health*, *17*(18), 6911. https://doi.org/10.3390/ijerph17186911
- Saeed, M., Alshammari, Y., Majeed, S. A., & Al-Nasrallah, E. (2020). Chemical Vapour Deposition of Graphene—Synthesis, Characterisation, and Applications: A Review. *Molecules*, *25*(17), 3856. https://doi.org/10.3390/molecules25173856
- Salih, E., Mekawy, M., Hassan, R. Y. A., & El-Sherbiny, I. M. (2016). Synthesis, characterization and electrochemical-sensor applications of zinc oxide/graphene oxide nanocomposite. *Journal of Nanostructure in Chemistry*, 6(2), 137-144. https://doi.org/10.1007/s40097-016-0188-z
- Satar, I., Sirajuddin, M. M., Permadi, A., & Latifatunnajib, S. (2023). Tofu wastewater (tww) treatment and hydrogen (h2) production by using a microbial electrolysis cell (mec) system. *Indonesian Journal of Environmental Management and Sustainability*, 7(1), 13-19. https://doi.org/10.26554/ijems.2023.7.1.13-19
- Vu, X., Armbruster, U., & Martin, A. (2016). Micro/mesoporous zeolitic composites: recent developments in synthesis and catalytic applications. *Catalysts*, 6(12), 183. https://doi.org/10.3390/catal6120183
- Xu, C., Wang, X., & Zhu, J. (2008). Graphene−metal particle nanocomposites. *The Journal of Physical Chemistry C*, 112(50), 19841-19845. https://doi.org/10.1021/jp807989b
- Yu, J., Wu, J., YU, S., Chen, S., Wang, R., & Zhang, X. (2022). Compensation of environmental parameters for optical detection of chemical oxygen demand. *Measurement Science and Technology,* 34(3), 035020. https://doi.org/10.1088/1361-6501/ac9e10
- Zhao, P. (2024). Alkaline chemical neutralization to treat acid mine drainage with high concentrations of iron and manganese. *Water*, 16(6), 821. https://doi.org/10.3390/w16060821